The redox properties of the Mn(II)/Mn(III) transition were further investigated by polarography in CH_2Cl_2. Plots of log $[i/(i_d - i)]$ vs E for the first reduction yield slopes that are acceptably close to the theoretical value of 59 mV for a one-electron transfer at 25 °C. This result was confirmed by differential-pulse polarography measurements in CH_2Cl_2 and $C_2H_4Cl_2$.[37] The half-widths of 88 and 110 mV in CH_2Cl_2 and $C_2H_4Cl_2$, respectively, leave little doubt about the presence of a one-electron process (for which a theoretical value of 90.4 mV is expected) rather than a two-electron step.[34] This behavior is consistent with a one-electron oxidation of the $[Mn(tdt)_2]^{2-}$ complex to a Mn(III) species, but all electrochemical data for **2** provide no evidence for the existence of any stable Mn(IV) species. Any tentative assignment of different oxidation states to the metal ions of the two chemically different complexes present in **2** can therefore be excluded.

The Pt electrode provides in all solvents much larger peak separations in the cyclic voltammograms of **2** than the glassy-carbon electrode. The same electrode effect on ΔE_p values was observed for the $[Mn_2(edt)_4]^{2-}$ ($[Mn(edt)_2(Me_2SO)_2]$)/$[Mn(edt)_2]^{2-}$ redox couple and assigned to a much smaller rate constant for the heterogeneous electron transfer at the Pt electrode.[35] Within the group of related M(II,III)/edt^{2-} and M(II,III)/tdt^{2-} complexes (M = Co, Fe, Mn), the manganese compounds exhibit the most pronounced electrode dependences in their CV characteristics. In addition, the ΔE_p values and redox potentials are strongly affected by the solvent. In CH_2Cl_2 (and in $C_2H_4Cl_2$) much smaller ΔE_p and less negative $E_{1/2}$ values are found than in DMF under similar conditions. The stronger interactions of better coordinating solvents (e.g. DMF vs CH_2Cl_2) with the planar $[Mn(tdt)_2]^-$ anions of **2** result in redox potentials that are more negative. The same arguments can be used to explain the smaller peak separation and the less cathodic potential for the Mn(II)/Mn(III) redox couple in DMF compared to Me_2SO.[35]

Acknowledgment. This work was supported by the Minister für Wissenschaft und Forschung des Landes Nordrhein-Westfalen, the Bundesminister für Forschung und Technologie (BMFT) under Contract No. 05339 GAB/3, and the Fonds der Chemischen Industrie. We are grateful to Dr. H. Strasdeit for valuable comments and discussions.

Supplementary Material Available: Positional and thermal parameters of the anions, cations, and solvate molecules (Tables S-I and S-IV), complete distances and angles within the anions, cations, and solvate molecules (Tables S-II and S-V), and details of data collection and structure refinements (Table S-VII) (19 pages); observed and calculated structure factors (Tables S-III and S-VI) (86 pages). Ordering information is given on any current masthead page.

---

[36] With the Pt-flag electrode another solvent-dependent reduction is seen at a very low potential (DMF, −1.80 V; CH_2Cl_2, −1.55 V) without any corresponding oxidation wave. In addition, a single oxidation wave at higher potential occurs (DMF, 0.33 V; CH_2Cl_2, 0.35 V).

[37] To exclude the possibility that CH_2Cl_2 may serve as a chloride donor for redox-active **2**, cyclic voltammograms and polarograms of **2** in 1,2-dichloroethane ($C_2H_4Cl_2$) and dichloromethane (CH_2Cl_2) were recorded. No substantial solvent-dependent differences, however, could be detected.

Contribution from the Departments of Chemistry, Thimann Laboratories, University of California,
Santa Cruz, California 95064, and University of California, Davis, California 95616

Novel Chiral Trinuclear and Symmetric Tetranuclear Imidazolate-Bridged Cobalt(III) Complexes of a Synthetic Analogue of Bleomycin

Steven J. Brown, Marilyn M. Olmstead,[†] and Pradip K. Mascharak*

Received January 17, 1989

Attempts to synthesize the cobalt(III) complex of PMAH (**2**), a designed ligand that mimics a major portion of the metal-chelating locus of the antitumor drug Bleomycin (BLM, **1**), have afforded two novel imidazolate-bridged trimeric and tetrameric complexes. The trimeric complex $[Co(L)]_3Cl(BF_4)_2{\cdot}9.25H_2O$ (**3**) (L = $PMAH_{-2H}$) crystallizes in the space group $R3$ with a = 40.838 (11) Å, c = 12.975 (3) Å, V = 18741 (8) Å^3, and Z = 12. The cation in **3** has 3-fold symmetry and is chiral. The chloride ion, which sits on the 3-fold axis, forms an intimate ion pair with the cation through hydrogen bonding. The tetrameric complex $[Co(L)]_4(BF_4)_4{\cdot}10DMF$ (**4**) crystallizes in the space group $P4/n$ with a = 21.436 (3) Å, c = 12.601 (3) Å, V = 5790 (2) Å^3, and Z = 2. In **4**, the cation has 4-fold symmetry and is optically inactive. The geometry at each cobalt(III) is approximately octahedral in both structures. Five nitrogen donor atoms from the doubly deprotonated ligand $PMAH_{-2}$ (L) occupy five coordination sites around each cobalt, while the sixth site is filled by the second nitrogen of the imidazole moiety of a neighboring unit. In aqueous and DMSO solutions, **3** exhibits strong CD signals. That both complex cations remain intact in solution has been checked by spectroscopic techniques including ^1H–^1H and ^1H–^{13}C COSY experiments. The structural and spectroscopic parameters of **3** and **4** are expected to provide help in elucidation of the structure(s) of Co^{III}–BLM.

Introduction

Bleomycins (BLM, **1**) are a family of glycopeptide antibiotics that are used in the treatment of certain types of cancer.[1] In the presence of a metal ion like Fe^{2+} and molecular oxygen, BLM inflicts single- and double-strand breaks in cellular DNA,[2-9] and the metal ion promoted DNA strand scission is assumed to be related to the drug action. Though the fact that metal chelates of BLM (metallobleomycins, M–BLMs) play a vital role in the complex drug–DNA chemistry is an accepted one, structural information on the architecture of the coordination spheres of the metal ions in M–BLMs remains rather elusive. Macromolecular M–BLMs have not been crystallized, and the coordination structures of M–BLMs have been predicted primarily on the basis of spectroscopic data.[2-9] In our "synthetic analogue approach"[10] to this problem, we are involved in determination of structures and reactivities of smaller model compounds (or analogues) that

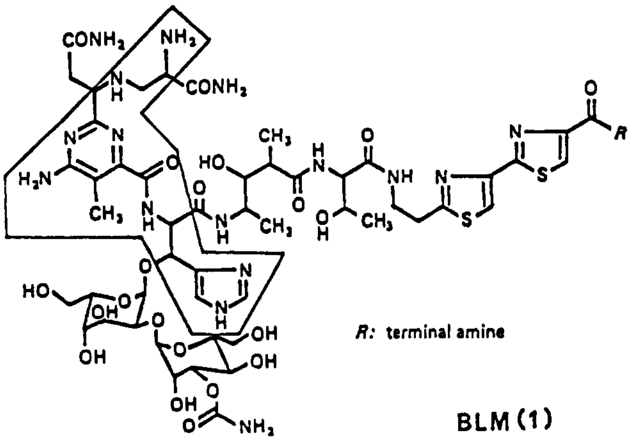

BLM (1)

---

* To whom correspondence should be addressed at the University of California, Santa Cruz.

[†] University of California, Davis.

mimic the various M–BLMs in terms of composition, redox state, and spectroscopic properties and that are also obtainable in crystalline form. As part of such pursuit, we have recently reported[11] the synthesis of a designed ligand PMAH (**2**; H refers to dissociable amide H) that mimics the major part of the metal-chelating locus of BLM (boxed area in **1**). We have also reported[11,12] the structure and spectroscopic properties of the copper(II) complex [Cu(PMA)]X (X = BF_4, ClO_4), which happens to be the first example of a crystalline analogue of a M–BLM. The results have contributed significantly to the understanding of the structural and reactivity parameters of Cu^{II}–BLM.

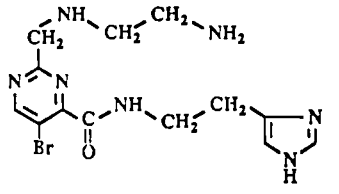

PMAH
(**2**)

Interest in various M–BLMs stems from the diverse biochemical characteristics of the metallodrugs. For example, Co^{III}–BLMs exhibit the unusual property of selective accumulation in the nuclei of certain types of cancer cells and hence radiolabeled $^{57}Co^{III}$–BLM has found diagnostic uses in nuclear medicine.[13] Also, it has been recently reported that Co^{III}–BLM can induce DNA strand breaks when illuminated with UV or visible light.[14,15] These results prompted us to explore the photochemistry of the Co(III) complex of PMAH. So far, our synthetic efforts have afforded, among other species, two novel polynuclear imidazolate-bridged Co(III) complexes. The first complex, $[Co(L)]_3Cl(BF_4)_2{\cdot}9.25H_2O$ (**3**, L = $PMAH_{-2H}$, i.e., doubly deprotonated PMAH[16]), is a chiral trimer, while the second one, $[Co(L)]_4(BF_4)_4{\cdot}10DMF$ (**4**), is a symmetric tetramer with no optical activity. We report in this paper the syntheses, structures, and spectral properties of these two cobalt complexes. Though our major thrust is directed toward characterization of the monomeric $[Co(PMA)S]^{2+}$ (S = solvent) unit[17] and its interaction with DNA, we completed studies on the structurally intriguing multinuclear species **3** and **4**, since they provide structural and spectral information pertinent to Co^{III}–BLM.

Experimental Section

Preparation of Compounds. PMAH (**2**) and $Na_3[Co(CO_3)_3]{\cdot}3H_2O$ were synthesized by following the published procedures.[11,18] The strongly acidic cation exchanger SP-C50-120 was purchased from Sigma Chemical Co.

$[Co(L)]_3Cl(BF_4)_2{\cdot}9.25H_2O$ (3) and $[Co(L)]_4(BF_4)_4{\cdot}10DMF$ (4) (L = $PMAH_{-2H}$). The trimer **3** and the tetramer **4** were isolated from the same reaction mixture. A typical synthesis is described below.

To a slurry of 300 mg (0.83 mmol) of $Na_3[Co(CO_3)_3]{\cdot}3H_2O$ in 10 mL of water was added a solution of 370 mg (1 mmol) of PMAH in 10 mL of water, and the mixture was stirred at room temperature for 6 h. It was then filtered to remove small amounts of a black residue. After the pH of the dark red filtrate was adjusted to ca. 3 with 2 N HCl, the solution was adsorbed onto a column of SP-C50-120 Sephadex cation-exchange resin (Na^+ form, length of column 20 cm). Elution with 0.2 N KCl solution caused two orange bands to move down the column, while a significant amount of dark brown material remained adsorbed at the top. The two batches of effluents containing the two bands were desalted by evaporating the orange solutions to dryness and extracting the complexes in ethanol. Evaporation of the ethanol extracts afforded orange powder for both bands.[19] The two complexes were then crystallized by following two different procedures. The orange powder from band 1 (the first one to come out of the column) was dissolved in 7 mL of water, and to this solution was added a solution of 100 mg of LiCl[20] and 250 mg of $LiBF_4$ in 3 mL of water. The mixture was then filtered to remove small amounts of KBF_4. The resultant orange filtrate, on slow evaporation, afforded 50 mg (overall yield 10%) of crystalline **3** (density 1.75 g cm^{-3}). The orange powder from band 2 was dissolved in 5 mL of water, and to this solution was added a solution of 200 mg of $LiBF_4$ in 2 mL of water. On slow evaporation of this orange aqueous solution, only needle-shaped crystals of the tetramer were obtained. Crystals suitable for X-ray studies (and composition **4**) were isolated by diffusion of diethyl ether into a solution of the needles in DMF. The overall yield of **4** was 8% (density 1.60 g cm^{-3}).

The synthetic procedure described above has been repeated eight times in this laboratory with reproducible results. Significant amounts (>250 mg) of both **3** and **4** have been obtained to complete structure determinations as well as the various physical measurements. Complexes **3** and **4** are therefore minor but nevertheless authentic products in the reaction between $Na_3[Co(CO_3)_3]{\cdot}3H_2O$ and PMAH in aqueous medium.[21]

The IR spectrum of **3** is identical with that of **4** except for the bands due to the solvent molecules of crystallization. Selected IR bands (KBr pellet, cm^{-1}): 3400 (m, br), 1607 (ν_{CO}, s), 1560 (s), 1490 (m), 1440 (w), 1388 (m), 1345 (m), 1246 (m), 1230 (m), 814 (w), 755 (m), 704 (w), 688 (w), 662 (w). Anal. Calcd for $C_{39}H_{66.5}N_{21}Co_3B_2Br_3ClF_8O_{12.25}$ (**3**): C, 28.35; H, 4.06; N, 17.82. Found: C, 28.65; H, 3.89; N, 18.07. Calcd for $C_{82}H_{134}N_{38}Co_4B_4Br_4F_{16}O_{14}$ (**4**): C, 35.42; H, 4.86; N, 19.16. Found: C, 35.67; H, 4.69; N, 18.97.

X-ray Data Collection, Structure Solution, and Refinement. For both complexes (**3** and **4**), diffraction data were collected at 130 K on a Syntex $P2_1$ diffractometer equipped with a graphite monochromator and a modified LT-1 low-temperature apparatus. Mo Kα radiation (λ = 0.71069 Å) was employed. Only random fluctuations of less than 2% were noted in the intensities of two standard reflections during the course of data collection in each case. The structures of the two complexes were solved by Patterson methods.[22,23] Hydrogen atoms bonded to the carbon atoms were included at calculated positions by using a riding model, with C–H of 0.96 Å and U_H of $1.2U_C$. The data were corrected for absorption effects by use of the program XABS.[24]

---

[1] Blum, R. H.; Carter, S. K.; Agre, K. A. *Cancer* **1973**, *31*, 903.

[2] Stubbe, J.; Kozarich, J. W. *Chem. Rev.* **1987**, *87*, 1107.

[3] Hecht, S. M. *Acc. Chem. Res.* **1986**, *19*, 383.

[4] Sugiura, T.; Takita, T.; Umezawa, H. *Met. Ions Biol. Syst.* **1985**, *19*, 81.

[5] Dabrowiak, J. C. *Adv. Inorg. Biochem.* **1983**, *4*, 69.

[6] Povrick, L. F. *Molecular Aspects of Anticancer Drug Action*; Neidle, S., Waring, M. J., Eds.; Macmillan: London, 1983; p 157.

[7] Dabrowiak, J. C. *Met. Ions. Biol. Syst.* **1980**, *11*, 305.

[8] Umezawa, H.; Takita, T. *Struct. Bonding (Berlin)* **1980**, *40*, 73.

[9] (a) *Bleomycin: Chemical, Biochemical and Biological Aspects*; Hecht, S. M., Ed.; Springer-Verlag: New York, 1979. (b) *Bleomycin: Current Status and New Developments*; Carter, S. K., Crooke, S. T., Umezawa, H., Eds.; Academic: New York, 1978.

[10] Ibers, J. A.; Holm, R. H. *Science (Washington, D.C.)* **1980**, *209*, 223.

[11] Brown, S. J.; Stephan, D. W.; Mascharak, P. K. *J. Am. Chem. Soc.* **1988**, *110*, 1996.

[12] Brown, S. J.; Hudson, S. E.; Stephan, D. W.; Mascharak, P. K. *Inorg. Chem.* **1989**, *28*, 468.

[13] (a) Rasker, J. J.; Van de Poll, M. A. P. C.; Beekhins, H.; Woldring, M. G.; Nieweg, H. O. *J. Nucl. Med.* **1975**, *16*, 1058. (b) Nouel, J. P. *Gann Monogr. Cancer Res.* **1976**, *19*, 301. (c) Nunn, A. D. *Int. J. Nucl. Med. Biol.* **1977**, *4*, 204. (d) Kono, A.; Matsushima, Y.; Kojima, M.; Maeda, T. *Chem. Pharm. Bull.* **1977**, *25*, 1725. (e) DeRiemer, L. H.; Meares, C. F.; Goodwin, D. A.; Diamanti, C. I. *J. Med. Chem.* **1979**, *22*, 1019. (f) Raban, P.; Brousil, J.; Svikovcova, P. *Eur. J. Nucl. Med.* **1979**, *4*, 191. (g) Kakinuma, J.; Kagiyama, R.; Orii, H. *Eur. J. Nucl. Med.* **1980**, *5*, 159.

[14] (a) Change, C.-H.; Meares, C. F. *Biochemistry* **1982**, *21*, 6332. (b) Chang, C.-H.; Meares, C. F. *Biochemistry* **1984**, *23*, 2268. (c) Subramanian, R.; Meares, C. F. *J. Am. Chem. Soc.* **1986**, *108*, 6427.

[15] (a) Suzuki, T.; Kuwahara, J.; Sugiura, Y. *Nucl. Acids Res.* **1984**, *15*, 161. (b) Suzuki, T.; Kuwahara, J.; Goto, M.; Sugiura, Y. *Biochim. Biophys. Acta* **1985**, *824*, 330.

[16] The two dissociable hydrogens are the amide H and the H on the pyrrole type nitrogen of the imidazole ring.

[17] Very recently, $[Co(PMA)S]^{2+}$ has been isolated in this laboratory. A report on its structure and reactivity parameters will appear elsewhere.

[18] Bauer, H. F.; Drinkard, W. C. *Inorg. Synth.* **1966**, *8*, 202.

[19] The IR spectra of these powders are identical with those of the final crystalline materials (**3** and **4**) except for bands due to the solvent molecules of crystallization.

[20] The Cl^- present in the crystals of **3** does not originate from this batch of LiCl, since the same crystals of **3** are isolated (in low yield) from identical attempts without LiCl. Addition of LiCl during crystallization improves the yield and also allows crystals to grow faster.

[21] The nature of the major product(s) in this reaction is under investigation at present.

[22] SHELXTL, Version 5, installed on a Data General Eclipse computer.

[23] Neutral-atom scattering factors and corrections for anomalous scattering were taken from: *International Tables for X-ray Crystallography*; Kynoch Press: Birmingham, England, 1974; Vol. IV.

Table I. Crystallographic Data

formula	$C_{39}H_{66.5}N_{21}Co_3B_2$-$Br_3ClF_8O_{12.25}$	$C_{82}H_{134}N_{38}Co_4B_4$-$Br_4F_{16}O_{14}$
mol wt	1651.17	2778.79
color and habit	red needles	red blocks
space group	*R*3 (No. 146)	*P*4/*n* (No. 85)
a, Å	40.838 (11)	21.436 (3)
c, Å	12.975 (3)	12.601 (3)
V, Å^3	18741 (8)	5790 (2)
Z	12	2
cryst dimens, mm	0.10 × 0.15 × 0.50	0.15 × 0.37 × 0.70
d_{calcd}(130 K), g cm^{-3}	1.76	1.59
d_{obsd}(298 K),[a] g cm^{-3}	1.75 (1)	1.60 (1)
μ(Mo Kα), cm^{-1}	28.2	20.2
transm coeff	0.68–0.79	0.56–0.73
scan method	ω, 0.8° range 0.8° offset for bkgd	ω, 1.2° range 1.0° offset for bkgd
2θ range, deg	0–50	0–50
no. of data collcd	8099	5665
no. of data in refinement	4335[$I > 3\sigma(I)$]	1550[$I > 3\sigma(I)$]
no. of params refined	554	191
R^b	0.059	0.092
$R_w{}^c$	0.062 [$w = 1/\sigma^2(F_o)$]	0.096 [$w = 1/\sigma^2(F_o)$]

[a] Determined by flotation in $CCl_4/CHBr_3$ and cyclohexane/$CHBr_3$, respectively. [b] $R = \sum|\Delta|/\sum|F_o|$. [c] $R_w = \sum(|\Delta|w^{1/2})/\sum(|F_o|w^{1/2})$, where $\Delta = |F_o| - |F_c|$.

The space group of the trimeric complex **3** was one of the five possible space groups, as indicated by the condition *hkl*, $-h + k + l = 3n$. A reasonable Patterson solution could only be obtained in *R*3. This noncentrosymmetric space group was reasonable in view of the circular dichroism exhibited by **3**. Location of all non-hydrogen atoms and most of the hydrogen atoms followed from successive least-squares refinement and calculation of difference maps. The asymmetric unit contains one trimeric cation with no crystallographically imposed symmetry and one Co-containing moiety arranged about a 3-fold axis (one-third of a trimer). Also contained in the asymmetric unit are one and one-third Cl^-, two and two-thirds of the BF_4^- groups, and twelve and one-third molecules of water. One of the BF_4^- groups is disordered such that three of the four fluorine atoms have two equally probable positions. Another BF_4^- group was assigned $^2/_3$ occupancy for the sake of charge balance. The handedness of the crystal was confirmed to correspond to the model chosen by a SHELXTL routine.[22] In the final cycles of refinement, hydrogen atoms were included (riding model) and anisotropic thermal parameters were assigned to Co, Cl, and Br atoms. The largest feature in the final difference map was 1.32 e Å^{-3} in height.

The space group of the tetrameric complex **4** was either *P*4/*n* (No. 85) or *P*4/*nmm* (No. 129), on the basis of the conditions *hk*0, $h + k = 2n$, and 0*k*0, $k = 2n$. The Laue symmetry indicated that the correct space group was probably *P*4/*n*, and the successful solution and refinement in this space group confirm its choice. Two molecules of DMF are disordered and situated on 4-fold axes. In the final cycles of refinement, hydrogen atoms were included as described above except for atoms in the two disordered molecules of DMF and for hydrogens bonded to the methyl groups of the other DMF molecules. Anisotropic thermal parameters were used for the Co and Br atoms. The largest peak on the final difference map was 1.37 e Å^{-3} in height.

Machine parameters, crystal data, and data collection parameters are summarized in Table I. Selected bond distances and angles for **3** and **4** are listed in Table II. The following data have been submitted as supplementary material: atomic coordinates and isotropic thermal parameters for the non-hydrogen atoms in **3** (Table S1) and **4** (Table S2), complete lists of bond lengths and angles for **3** (Tables S3 and S4) and **4** (Tables S7 and S8), anisotropic thermal parameters for **3** (Table S5) and **4** (Table S9), H atom coordinates and isotropic thermal parameters for **3** (Table S6) and **4** (Table S10), and values of 10$|F_o|$ and 10$|F_c|$ (Tables S11 and S12).

Other Physical Measurements. Infrared spectra were obtained with a Perkin-Elmer 1600 FTIR spectrometer. Absorption spectra were measured on a Perkin-Elmer Lambda 9 spectrophotometer. ^1H and ^{13}C NMR spectra were recorded on a General Electric 300-MHz GN-300 instrument. Samples were dissolved in $(CD_3)_2SO$ (99.5% D). Multiplicities of ^{13}C NMR peaks were determined from APT and DEPT data. Standard pulse sequences[25] were used to obtain ^1H–^1H and ^1H–^{13}C two-dimensional scalar-correlated NMR spectra. The experimental details have already been published.[26] Circular dichroism (CD) spectra were obtained with an AVIV Model 60DS CD spectrometer. Elemental analysis were performed by Atlantic Microlab Inc., Atlanta, GA.

Results and Discussion

Syntheses of Co(III) complexes via aerobic oxidation of mixtures of Co(II) salts and the appropriate ligands are usually beset with problems associated with complicated consecutive reactions leading to superoxo and binuclear peroxo complexes.[27] Attempts to synthesize the Co(III) complex(es) of PMAH from Co(II) sources were particularly frustrating in this regard; the reaction mixtures invariably turned deep brown, showing formation of such oxygenated species, and no tractable solid product was isolated from these brown solutions. Following several unsuccessful attempts, the other general method of substitution between a starting Co(III) complex and a multidentate ligand[28] was tried. Among the few convenient Co(III) starting complexes, the green tris(carbonato)cobaltate(III) anion has often been the material of choice, since substitution of the carbonate groups can be easily controlled by the kind and amount of the incoming ligand and by temperature and other parameters.[29] In the present work, use of $Na_3[Co(CO_3)_3]\cdot3H_2O$ also allowed us to isolate two complexes of PMAH, namely **3** and **4**. Addition of PMAH to a slurry of $Na_3[Co(CO_3)_3]\cdot3H_2O$ in water results in a rapid color change of green to orange, indicating formation of a $Co^{III}N_6$ chromophore. As described in the Experimental Section, the orange solution eventually affords the complexes **3** and **4** along with some unknown products.

In the present synthetic procedure, imidazolate-bridged species (**3** and **4**) appear to form quite readily, since (a) Co(III) almost exclusively prefers six-coordination and PMAH offers five donor centers to one metal ion and (b) the basicity of the initial reaction mixture causes deprotonation of the NH group of the imidazole moiety,[30,31] and renders the nitrogen ready for coordination. Solution studies on metal complexes of glycyl-L-histidine have indicated formation of tetramers following ionization at the unbound imidazole of the histidine residue,[32] and the recently reported imidazole-bridged Co(III) amine complexes[33] clearly demonstrate the tendency toward olgiomerization of coordinatively unsaturated Co(III) centers through imidazolate bridging. Taken together, these results suggest that the mononuclear Co(III) complex could be isolated better as $[Co(PMA)L]^{n+}$ (n = 1 or 2) with additional ligand L (to occupy the sixth coordination site on cobalt) present in the reaction mixture. Such attempts are in progress.

The coordination chemistry of cobalt–BLM is rather extensive.[4-8,34] Aerobic oxidation of Co^{II}–BLM gives rise to at least three different products.[13e] Among them, the so-called brown and green Co^{III}–BLMs are believed to contain superoxo and hydroperoxo groups bound to cobalt, while the thermodynamically stable orange Co^{III}–BLM is reported to contain no "active" form of dioxygen in the coordination sphere of the metal. Five N donors from the primary and secondary amine groups, pyrimidine and imidazole rings, and the amide moiety of BLM (**1**) and a hereto unknown ligand have been proposed to occupy the six coordination sites around cobalt in orange Co^{III}–BLM.[2,5] As discussed in the next section, the coordination sphere around each cobalt center in both **3** and **4** resembles this description of the coordination structure of orange Co^{III}–BLM rather closely. Interst in **3** and

---

(24) Moezzi, B. Ph.D. Dissertation, University of California, Davis, 1987.

(25) Benn, R.; Gunther, H. *Angew. Chem., Int. Ed. Engl.* **1983**, *48*, 350.

(26) Delany, K.; Arora, S. K.; Mascharak, P. K. *Inorg. Chem.* **1988**, *27*, 705.

(27) Cotton, F. A.; Wilkinson, G. In *Advanced Inorganic Chemistry*, 5th ed.; Wiley: New York, 1988; pp 735–738.

(28) Buckingham, D. A.; Clark, C. R. In *Comprehensive Coordination Chemistry*; Wilkinson, G., Ed.; Pergamon: Oxford, 1987; Vol. 4, p 635.

(29) Shibata, M. *Top. Curr. Chem.* **1983**, *110*, 26.

(30) The pK_a of the NH group of imidazole coordinated to Co(III) has been estimated to be close to 11.[31]

(31) (a) Harrowfield, J. M.; Norris, V.; Sargeson, A. M. *J. Am. Chem. Soc.* **1976**, *98*, 7282. (b) Brodsky, N. R.; Nguyen, N. M.; Rowan, N. S.; Storm, C. B.; Butcher, R. J.; Sinn, E. *Inorg. Chem.* **1984**, *23*, 891.

(32) Morris, P. J.; Martin, R. B. *J. Inorg. Nucl. Chem.* **1971**, *33*, 2913.

(33) Hawkins, C. J.; Horn, E.; Martin, J.; Palmer, J. A. L.; Snow, M. R. *Aust. J. Chem.* **1986**, *39*, 1213.

(34) For a compilation of representative papers in this area, see ref 26.

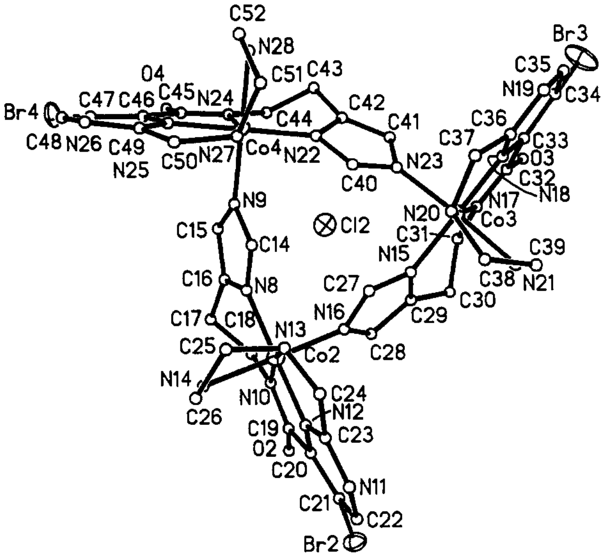

Figure 1. Computer-generated drawing of the type A cation in **3** with the atom-labeling scheme. Atoms that have been refined anisotropically are represented by thermal ellipsoids (probability level 50%). The average Co···Co distance is 5.858 (1) Å.

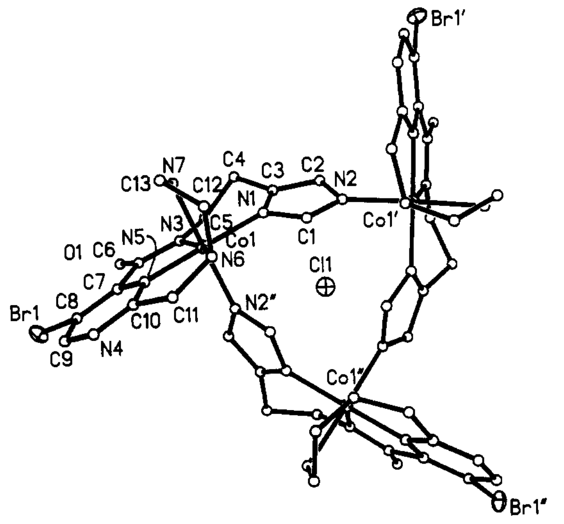

Figure 2. Computer-generated drawing of the type B cation in **3** with the atom-labeling scheme. 50% thermal ellipsoids have been used for atoms refined anisotropically. The Co···Co distance is 5.843 (1) Å.

4 therefore extends beyond the novelty of the structures of these two complexes.

Structure of [Co(L)]$_3$Cl(BF$_4$)$_2$·9.25H$_2$O (3). The unit cell contains twelve formula units. Nine of the trimeric cations (type A) have approximate 3-fold symmetry, and the remaining three (type B) have crystallographic 3-fold symmetry. The approximate 3-fold axis is tipped 34° with respect to the *a* direction of the crystal, while the crystallographic 3-fold axis is parallel to *c*. Both type A and B cations have the same chirality. Figures 1 and 2 illustrate the numbering scheme and the similar conformations for the two types of cations as viewed down the 3-fold axes. Though the tetrafluoroborates are essentially noninteracting, each trimeric cation forms an intimate ion pair with one chloride ion trapped into a pocket formed by the propeller-like arrangement of the ligands. In the type B pair, the chloride ion lies on the crystallographic 3-fold axis with a Co···Cl distance of 4.713 Å; in the type A pair, three similar Co···Cl distances of 4.832, 4.805, and 4.769 Å are observed. The chloride ion has short contacts to the secondary amine hydrogens (range 2.35–2.77 Å), to the hydrogens of the imidazole carbon that is bracketed by two nitrogens (range 2.48–2.79 Å), and presumably to the hydrogens of the water molecules (Cl···O distances from 2.98 to 3.26 Å). There are eight such interactions for Cl(1) and nine for Cl(2).

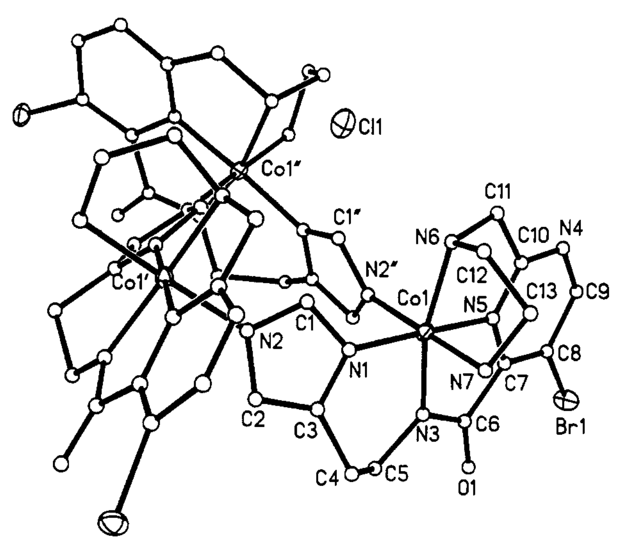

Figure 3. Perspective drawing of the type B cation showing the open side of the trimer and the position of the chloride ion. The view is approximately perpendicular to the 3-fold axis.

Shown in Figure 3 is the type B ion pair with a view of the trapped chloride ion approximately perpendicular to the 3-fold axis. A considerable amount of water is also present in the structure, a total of 111 molecules in the unit cell (9.25 molecules per trimer). As expected, the water molecules are all within hydrogen-bonding distances.

The donor set for each of the three octahedrally coordinated Co(III) ions consists of five nitrogen atoms from the ligand L (PMAH$_{-2H}$[16]) and a sixth nitrogen from the imidazolate moiety of a neighboring unit in the trimeric species (Figures 1 and 2). Selected bond distances and angles are collected in Table II. The average Co(III)–N$_{pm}$ (pm = pyrimidine), Co(III)–N$_{im}$ (im = imidazolato), and Co(III)–N$_{pep}$ (pep = peptide) bonds in **3** are respectively 1.866 (15), 1.924 (15), and 1.920 (15) Å long. These bond lengths compare well with those observed in the "bis" complex [Co(Prpep)$_2$]ClO$_4$·2.25H$_2$O (**6**),[35,36] where PrpepH is the tridentate peptide ligand **5** (H is the dissociable amide H). For

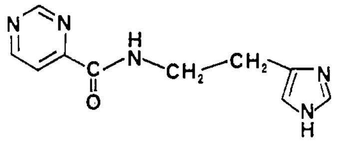

PrpepH (5)

example, the Co(III)–N$_{pep}$ bond in **6** is 1.927 (5) Å long. The Co(III)–N$_{pm}$ bond in **3** is slightly shorter than that in **6** (1.943 (5) Å) due to the fact that, unlike that of **5**, the pyrimidine ring of PMAH (**2**) becomes part of two five-membered chelate rings in both **3** and **4** and, consequently, the pyrimidine N is drawn closer to the cobalt centers in these two complexes. There are two types of Co(III)–N$_{im}$ bonds in **3** (and **4**). For the first type, which consists of Co(III)–N$_{im}$ bonds within a [CoL] unit, the average bond length (1.924 (15) Å) is quite close to the Co(III)–N(imidazole) bond distance (1.931 (5) Å) recorded for **6**. It should be noted, however, that in **6** the ligand framework contains an *imidazole* moiety as compared to the *imidazolate* group present in **3** (and **4**). The second type of Co(III)–N$_{im}$ bonds that connect [CoL] units in **3** (and **4**) are expectedly longer (average 1.957 (15) Å). Similar behavior (two different M–N-

---

(35) Muetterties, M.; Cox, M. B.; Arora, S. K.; Mascharak, P. K. *Inorg. Chim. Acta* **1989**, *160*, 123.

(36) It is interesting to note that like the Prpep$^-$ ligand, which occupies three coordination sites in a plane ([Co(Prpep)$_2$]$^+$ is isolated only as the mer isomer), the pyrimidine, peptide, and imidazole nitrogens of PMAH all lie in a plane around cobalt in **3** (and **4**).

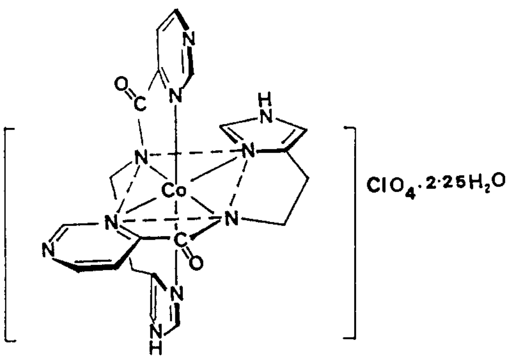

(6)

(imidazolato) bond lengths) has been observed with other imidazolate-bridged complexes.[33,37,38] The dimensions of the imidazolate rings in 3 (and 4) are also comparable to those observed in complexes reported previously. The Co(III)–NH_2 and Co(III)–NH bond lengths in 3 (and 4) fall within the range (1.85–2.10 Å) noted for various triethylenetetramine[39] and tetraethylenepentamine[40] complexes of tervalent cobalt. Significant deviations from 90° are observed with the N–Co–N angles in the five-membered chelate rings. The remaining angles in the structure more closely approach the expected values, however.

Structure of [Co(L)]$_4$(BF$_4$)$_4$·10DMF (4). The structure of the tetrameric cation in 4 is closely related to the trimeric one of 3 due to the fact that the coordination geometry, the set of donor atoms, and the disposition of the ligand framework around each cobalt atom are identical in the two species. However, the point symmetry of the cation is $4/m$ rather than 3, and there is no open side as there is for the trimer. A computer-generated drawing of the cation with the numbering scheme is shown in Figure 4, and selected structural parameters are listed in Table II. There is no chloride in this structure; electroneutrality is achieved by the presence of four BF_4^- ions. Extra room in the structure is filled by DMF molecules instead of water. The secondary amine group of the ligand is hydrogen-bonded to the oxygen atom of one DMF moelcule (N(6)···O(2) = 2.802 Å). Similarities in metric features of the coordination structures of cobalt(III) in 3 and 4 have already been discussed.

Figures 1, 2, and 4 illustrate the presence of open space in the central regions of the cations of 3 and 4. However, when all the hydrogen atoms that belong to atoms in the central regions are included through use of the program SPACFIL,[41] it becomes evident that there is little room left for a "guest" atom or molecule at the center. The two SPACFIL drawings have been deposited as supplementary material (Figures S1 and S2). In 3, the hydrogen atoms in the cavity are the imidazole hydrogens that make relatively short contacts to the chloride ion (~2.5 Å). In 4, the relevant hydrogens are the methylene hydrogens of C(4) and C(5). Clearly, 4 has a more hydrophobic interior. Despite scarcity of space at the very center of the cations, both structures do offer pockets of certain shapes to docking species. In the case of 3, the pocket is also chiral. On the basis of these characteristics, use of these pockets in "host-guest chemistry"[42] is anticipated and appropriate studies are in progress in this laboratory.

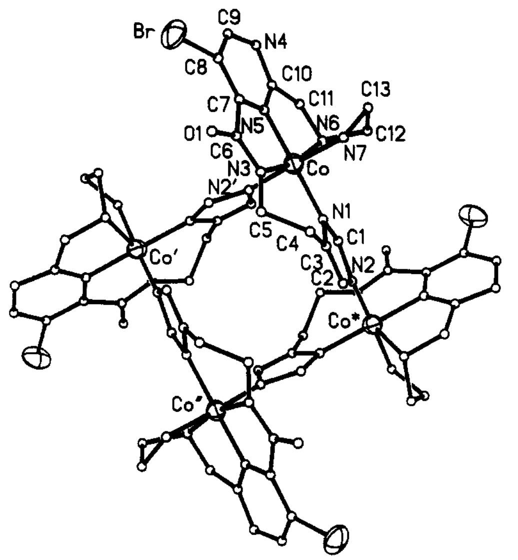

Figure 4. Computer-generated drawing of the cation in 4. Anisotropically refined atoms are shown with 50% thermal ellipsoids. The Co···Co distance is 5.896 (1) Å.

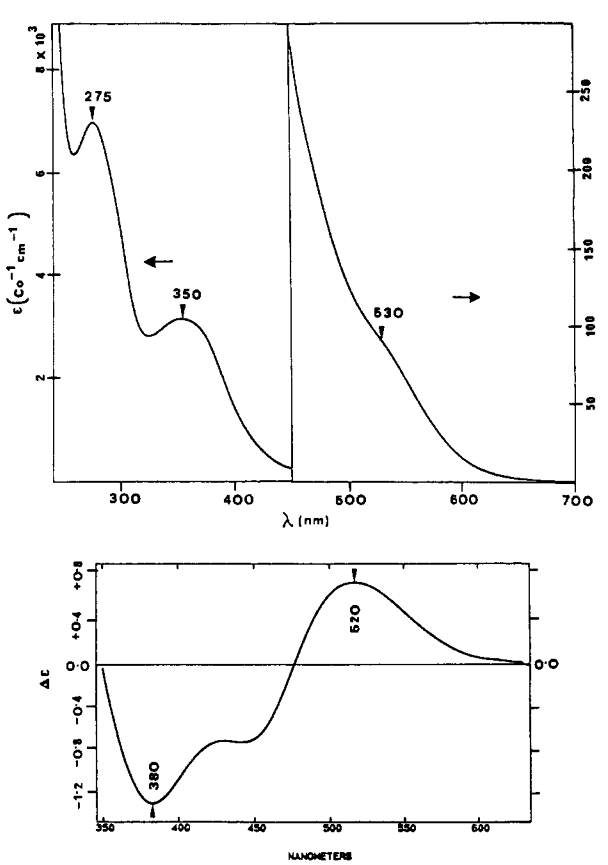

Figure 5. Electronic absorption spectrum (top) and circular dichroism spectrum (bottom) of 3 in water. The ε values are quoted as liter per mole of cobalt per centimeter.

Properties. Crystals of 3 and 4 dissolve in water, DMSO, and DMF to give orange-yellow solutions. The electronic absorption spectra of these two complexes[43] (Figure 5, Table III) consists

---

(37) Davis, W. M.; Dewan, J. C.; Lippard, S. J. *Inorg. Chem.* **1981**, *20*, 2928 and references cited therein.

(38) (a) Sundberg, R. J.; Martin, R. B. *Chem. Rev.* **1974**, *74*, 471. (b) Drew, M. G. B.; McCann, M.; Nelson, S. M. *J. Chem. Soc., Dalton Trans.* **1981**, 1868. (c) Matsumoto, K.; Ooi, S.; Nakao, Y.; Mori, W.; Nakahara, A. *J. Chem. Soc., Dalton Trans.* **1981**, 2045. (d) Costes, J. P.; Serra, J. F.; Dahan, F.; Laurent, J. P. *Inorg. Chem.* **1986**, *25*, 2790. (e) Matsumoto, N.; Yamashita, S.; Ohyoshi, A.; Kohata, S. Okawa, H. *J. Chem. Soc., Dalton Trans.* **1988**, 1943.

(39) (a) Freeman, H. C.; Maxwell, I. E. *Inorg. Chem.* **1970**, *9*, 649. (b) Freeman, H. C.; Marzilli, L. G.; Maxwell, I. E. *Inorg. Chem.* **1970**, *9*, 2408. (c) Buckingham, D. A.; Maxwell, I. E.; Sargeson, A. M.; Snow, M. R. *J. Am. Chem. Soc.* **1970**, *92*, 3617. (d) Buckingham, D. A.; Marzilli, L. G.; Sargeson, A. M.; Turnbull, K. R. *J. Am. Chem. Soc.* **1974**, *96*, 1713.

(40) (a) Snow, M. R. *J. Am. Chem. Soc.* **1970**, *92*, 3610. (b) Snow, M. R. *J. Chem. Soc., Dalton Trans.* **1972**, 1627.

(41) Wipke, W. T. In *Computers from A-Z: A Manufacturer's Guide to Hardware/Software for the Pharmaceutical Laboratory*; Aster Publishing: Springfield, OR, 1984.

(42) (a) Cram, D. J.; Trueblood, K. N. *Top. Curr. Chem.* **1981**, *98*, 43. (b) Cram, D. J. *Science* (*Washington, D.C.*) **1988**, *240*, 760.

(43) When the concentrations are normalized to per mole of cobalt, the electronic spectra of 3 and 4 are essentially identical with one another.

Table II. Selected Bond Distances (Å) and Angles (deg) for Compounds **3** and **4**[a]

$[Co(L)]_3Cl(BF_4)_2\cdot 9.25H_2O$ (**3**)[b]							
Br(1)–C(8)	1.849 (18)	Co(1)–N(1)	1.929 (14)	N(5)–C(7)	1.360 (23)	N(5)–C(10)	1.306 (20)
Co(1)–N(3)	1.913 (14)	Co(1)–N(5)	1.859 (13)	N(6)–C(11)	1.504 (20)	N(6)–C(12)	1.434 (24)
Co(1)–N(6)	2.022 (14)	Co(1)–N(7)	1.960 (17)	N(7)–C(13)	1.521 (22)	C(2)–C(3)	1.362 (30)
Co(1)–N(2)′	1.966 (10)	O(1)–C(6)	1.243 (20)	C(3)–C(4)	1.513 (32)	C(4)–C(5)	1.548 (22)
N(1)–C(1)	1.352 (26)	N(1)–C(3)	1.334 (21)	C(6)–C(7)	1.512 (21)	C(7)–C(8)	1.370 (23)
N(2)–C(1)	1.350 (21)	N(2)–C(2)	1.346 (26)	C(8)–C(9)	1.459 (23)	C(10)–C(11)	1.477 (28)
N(3)–C(5)	1.504 (21)	N(3)–C(6)	1.347 (20)	C(12)–C(13)	1.485 (35)		
N(4)–C(9)	1.329 (25)	N(4)–C(10)	1.294 (22)				
N(1)–Co(1)–N(3)	95.0 (6)	N(1)–Co(1)–N(5)	177.5 (6)	Co(1)–N(6)–C(11)	107.0 (10)	Co(1)–N(6)–C(12)	107.4 (12)
N(3)–Co(1)–N(5)	83.0 (6)	N(1)–Co(1)–N(6)	98.5 (6)	C(11)–N(6)–C(12)	113.0 (16)	Co(1)–N(7)–C(13)	109.3 (12)
N(3)–Co(1)–N(6)	165.5 (7)	N(5)–Co(1)–N(6)	83.7 (6)	N(1)–C(1)–N(2)	110.1 (14)	N(2)–C(2)–C(3)	108.6 (15)
N(1)–Co(1)–N(7)	89.1 (6)	N(3)–Co(1)–N(7)	89.8 (6)	N(1)–C(3)–C(2)	108.4 (18)	N(1)–C(3)–C(4)	120.6 (18)
N(5)–Co(1)–N(7)	92.3 (7)	N(6)–Co(1)–N(7)	85.0 (6)	C(2)–C(3)–C(4)	130.7 (15)	C(3)–C(4)–C(5)	112.9 (16)
N(1)–Co(1)–N(2)′	89.5 (6)	N(3)–Co(1)–N(2)′	91.6 (6)	N(3)–C(5)–C(4)	109.6 (14)	O(1)–C(6)–N(3)	126.6 (13)
N(5)–Co(1)–N(2)′	89.1 (6)	N(6)–Co(1)–N(2)′	93.9 (6)	O(1)–C(6)–C(7)	121.9 (14)	N(3)–C(6)–C(7)	111.5 (14)
N(7)–Co(1)–N(2)′	178.1 (6)	Co(1)–N(1)–C(1)	125.5 (10)	N(5)–C(7)–C(6)	111.2 (13)	N(5)–C(7)–C(8)	118.7 (15)
Co(1)–N(1)–C(3)	126.2 (13)	C(1)–N(1)–C(3)	106.6 (15)	C(6)–C(7)–C(8)	130.0 (16)	Br(1)–C(8)–C(7)	127.2 (13)
C(1)–N(2)–C(2)	106.0 (17)	C(1)–N(2)–Co(1)″	124.2 (13)	Br(1)–C(8)–C(9)	117.0 (12)	C(7)–C(8)–C(9)	115.8 (16)
C(2)–N(2)–Co(1)″	129.9 (12)	Co(1)–N(3)–C(5)	126.6 (12)	N(4)–C(9)–C(8)	121.8 (15)	N(4)–C(10)–N(5)	125.3 (17)
Co(1)–N(3)–C(6)	116.3 (10)	C(5)–N(3)–C(6)	116.8 (13)	N(4)–C(10)–C(11)	121.2 (15)	N(5)–C(10)–C(11)	113.4 (15)
C(9)–N(4)–C(10)	117.4 (15)	Co(1)–N(5)–C(7)	117.7 (10)	N(6)–C(11)–C(10)	112.7 (15)	N(6)–C(12)–C(13)	109.9 (15)
Co(1)–N(5)–C(10)	120.7 (13)	C(7)–N(5)–C(10)	121.0 (14)	N(7)–C(13)–C(12)	105.7 (18)		
$[Co(L)]_4(BF_4)_4\cdot 10DMF$ (**4**)[c]							
Br–C(8)	1.881 (20)	Co–N(1)	1.937 (13)	N(7)–C(13)	1.516 (23)	C(2)–C(3)	1.311 (23)
Co–N(3)	1.976 (16)	Co–N(5)	1.887 (12)	C(3)–C(4)	1.438 (28)	C(4)–C(5)	1.543 (25)
Co–N(6)	2.001 (14)	Co–N(7)	1.964 (14)	C(6)–C(7)	1.466 (25)	C(7)–C(8)	1.395 (24)
Co–N(2)′	1.928 (14)	O(1)–C(6)	1.257 (25)	C(8)–C(9)	1.408 (29)	C(10)–C(11)	1.534 (27)
N(1)–C(1)	1.332 (24)	N(1)–C(3)	1.385 (23)	C(12)–C(13)	1.461 (29)	O(2)–C(14)	1.210 (30)
N(2)–C(1)	1.383 (20)	N(2)–C(2)	1.353 (26)	N(8)–C(14)	1.386 (34)	N(8)–C(15)	1.490 (35)
N(3)–C(5)	1.393 (23)	N(3)–C(6)	1.322 (22)	N(8)–C(16)	1.447 (31)	O(3)–C(17)	1.193 (27)
N(4)–C(9)	1.348 (26)	N(4)–C(10)	1.367 (22)	N(9)–C(17)	1.339 (31)	N(9)–C(18)	1.486 (39)
N(5)–C(7)	1.341 (23)	N(5)–C(10)	1.281 (24)	N(9)–C(19)	1.506 (31)		
N(6)–C(11)	1.468 (20)	N(6)–C(12)	1.505 (22)				
		N(1)–Co–N(3)	94.3 (6)	Co–N(7)–C(13)	109.8 (11)	N(1)–C(1)–N(2)	110.0 (16)
N(1)–Co–N(5)	177.0 (7)	N(3)–Co–N(5)	82.9 (6)	N(2)–C(2)–C(3)	113.5 (16)	N(1)–C(3)–C(2)	105.6 (16)
N(1)–Co–N(6)	99.1 (6)	N(3)–Co–N(6)	165.3 (5)	N(1)–C(3)–C(4)	120.5 (14)	C(2)–C(3)–C(4)	133.8 (18)
N(5)–Co–N(6)	83.6 (6)	N(1)–Co–N(7)	87.9 (6)	C(3)–C(4)–C(5)	115.6 (17)	N(3)–C(5)–C(4)	110.5 (15)
N(3)–Co–N(7)	89.9 (6)	N(5)–Co–N(7)	90.9 (6)	O(1)–C(6)–N(3)	124.6 (17)	O(1)–C(6)–C(7)	120.2 (16)
N(6)–Co–N(7)	84.6 (6)	N(1)–Co–N(2)′	90.1 (6)	N(3)–C(6)–C(7)	115.2 (17)	N(5)–C(7)–C(6)	113.2 (14)
N(3)–Co–N(2)′	93.2 (6)	N(5)–Co–N(2)′	91.2 (5)	N(5)–C(7)–C(8)	113.5 (16)	C(6)–C(7)–C(8)	133.1 (17)
N(6)–Co–N(2)′	92.8 (6)	N(7)–Co–N(2)′	176.4 (6)	Br–C(8)–C(7)	123.9 (15)	Br–C(8)–C(9)	117.7 (14)
Co–N(1)–C(1)	127.2 (12)	Co–N(1)–C(3)	124.5 (12)	C(7)–C(8)–C(9)	118.3 (18)	N(4)–C(9)–C(8)	126.4 (17)
C(1)–N(1)–C(3)	107.8 (13)	C(1)–N(2)–C(2)	103.1 (14)	N(4)–C(10)–N(5)	126.8 (18)	N(4)–C(10)–C(11)	117.9 (16)
C(1)–N(2)–Co′	127.2 (14)	C(2)–N(2)–Co′	129.3 (11)	N(5)–C(10)–C(11)	115.3 (15)	N(6)–C(11)–C(10)	108.6 (15)
Co–N(3)–C(5)	124.5 (12)	Co–N(3)–C(6)	112.5 (12)	N(6)–C(12)–C(13)	106.9 (15)	N(7)–C(13)–C(12)	105.9 (14)
C(5)–N(3)–C(6)	123.0 (16)	C(9)–N(4)–C(10)	109.6 (16)	C(14)–N(8)–C(15)	116.1 (20)	C(14)–N(8)–C(16)	119.3 (21)
Co–N(5)–C(7)	115.8 (11)	Co–N(5)–C(10)	118.7 (12)	C(15)–N(8)–C(16)	122.3 (21)	O(2)–C(14)–N(8)	122.3 (21)
C(7)–N(5)–C(10)	125.2 (14)	Co–N(6)–C(11)	110.2 (10)	C(17)–N(9)–C(18)	119.9 (21)	C(17)–N(9)–C(19)	120.0 (20)
Co–N(6)–C(12)	107.2 (12)	C(11)–N(6)–C(12)	113.1 (12)	C(18)–N(9)–C(19)	120.1 (22)	O(3)–C(17)–N(9)	125.8 (21)

[a] For a complete listing, see Tables S3, S4, S7, and S8 (supplementary material). [b] Symmetry codes: ′ = $1 - x + y$, $1 - x$, z; ″ = $1 - y$, $x - y$, z. [c] Symmetry codes: ′ = $1 - y$, $^1/_2 + x$, $1 - z$; ″ = $y - {}^1/_2$, $1 - x$, $1 - z$.

of a moderately strong ($\epsilon \sim 3000$ L (mol of Co)$^{-1}$ cm^{-1}) band at 350 nm with a well-defined shoulder at ~530 nm ($\epsilon = 100$ L (mol of Co)$^{-1}$ cm^{-1}). In water, both **3** and **4** exhibit another strong band ($\epsilon \sim 7000$ L (mol of Co)$^{-1}$ cm^{-1}) with maximum (λ_{max}) at 275 nm. For low-spin octahedral Co(III), two spin-allowed d–d transitions, namely ${}^1A_{1g} \rightarrow {}^1T_{1g}$ and ${}^1A_{1g} \rightarrow {}^1T_{2g}$, are expected. Complexes with a $Co^{III}N_6$ chromophore usually display an absorption band with λ_{max} in the region 450–500 nm ($\epsilon \sim$ 10–300 M^{-1} cm^{-1}), which corresponds to the ${}^1A_{1g} \rightarrow {}^1T_{1g}$ transition.[44] For example, **6**[35] and a closely related complex[26] each exhibit an absorption band with λ_{max} at ~500 nm, which has been assigned to the ${}^1A_{1g} \rightarrow {}^1T_{1g}$ transition. The same transition gives rise to an absorption band at 452 nm ($\epsilon \sim 200$) with a shoulder at 520 nm in orange Co^{III}–BLM.[13e,45] We tentatively assign the ~525-nm absorptions of **3** and **4** to the ${}^1A_{1g} \rightarrow {}^1T_{1g}$ transition. Close association of this absorption with the strong band at 350 nm does not allow us to comment further, particularly in the absence of any Gaussian analysis of the absorption envelopes of the present complexes. The 350-nm bands of **3** and **4** are too strong for a d–d absorption band and must arise from charge-transfer absorption. They appear to be associated with the pyrimidine and the amido groups of the complexes, since **6** exhibits a ligand-to-metal charge-transfer (LMCT) band at 330 nm.[26,35] Interestingly, a 325-nm band ($\epsilon = 6500$ M^{-1} cm^{-1}) in the absorption spectrum of the Co(III) complex of the pseudotetrapeptide of BLM (**7**) has also been suggested to have a similar charge-transfer origin.[46] The second d–d transition (${}^1A_{1g} \rightarrow {}^1T_{2g}$), which is also expected in the 350–400-nm region, might be hidden under the 350-nm bands of **3** and **4** (Figure 5). The 270-nm band is likely to arise from electronic transition(s) associated with the bound pyrimidine function.[46]

It is important to note here that the proposed set of donor atoms around cobalt in **7**[46] differs from those in **3** and **4** (Figures 1, 2,

---

(44) Lever, A. B. P. In *Inorganic Electronic Spectroscopy*, 2nd ed.; Elsevier: Amsterdam, 1984; pp 463–478.

(45) Chang, C. H.; Dallas, J. L.; Meares, C. F. *Biochem. Biophys. Res. Commun.* **1983**, *110*, 959.

(46) Dabrowiak, J. C.; Tsukayama, M. *J. Am. Chem. Soc.* **1981**, *103*, 7543.

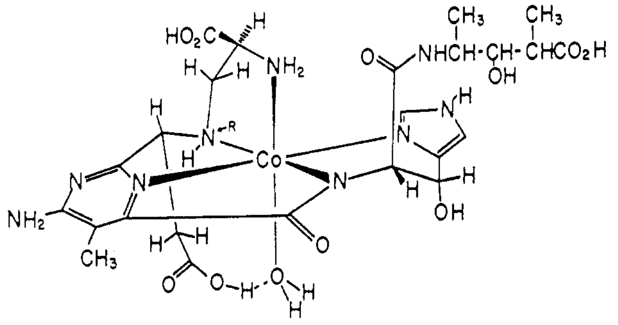

(7)

and 4) by only one entry. In **7**, the sixth ligand is H_2O, while the same site is occupied by an imidazolate nitrogen in both **3** and **4**. The larger magnitude of the crystal field due to replacement of H_2O by the imidazolate ligand is presumably reflected in the blue shift of the first d–d band (530 nm for **3** and **4**, 550 nm for **7**). Compared to PMAH (**2**), the pseudotetrapeptide A of BLM is a more crowded ligand. Additional organic moieties on the ligand framework as well as different substituents on the pyrimidine ring might account for the fact that the electronic spectrum of **7** is somewhat different from those of **3** and **4** (Table III). Unfortunately, such arguments cannot be extended all the way to orange Co^{III}–BLM, since (a) the structural relationship between orange Co^{III}–BLM and its acid hydrolysis product **7** is unknown[2,7] and (b) the reported electronic spectrum of orange Co^{III}–BLM[13e,45] is again different from that of **7**. As a consequence, the architecture of the coordination sphere around cobalt in orange Co^{III}–BLM remains rather obscure at present.

The circular dichroism (CD) spectrum of **3** in water is shown in Figure 5, and the spectral parameters are listed in Table III. Since we did not determine the absolute stereochemistry of the chiral trimeric cation in **3** by crystallography, no attempt has been made to correlate the CD spectrum with the absolute configuration of the optically active species. The large positive Cotton effect at ~520 nm and the small negative CD band around 450 nm appear to arise from the two d–d transitions, while the large negative peak at 380 nm could be attributed to the charge-transfer transition involving the bound pyrimidine and the peptido group of the complex. The CD spectrum of **3** in DMSO is very similar to that shown in Figure 5. So far, we have been successful in isolating one optical isomer of **3** under the reaction conditions described in the Experimental Section. The isomer with opposite chirality is presumably retained on the column along with other products of the reaction.

NMR Spectra. The ^1H and ^{13}C NMR spectra of **3** in $(CD_3)_2SO$ are shown in Figure 6, and the various peak positions are listed in Table III. In Figure 6 (and the following figures), resonances corresponding to the various hydrogen and carbon atoms of the complex have been labeled in accordance with Figure 2. Both ^1H–^1H and ^1H–^{13}C COSY results (vide infra) as well as APT and DEPT data have been used to assign these resonances. In three independent measurements, the NMR samples exhibited the same CD spectra, which in turn are very similar to the one recorded for **3** in water. The trimeric structure (Figures 1 and 2), therefore, remains intact in DMSO solution.

The presence of imidazolate bridges in **3** is clearly evident by the absence of the imidazole NH peak, which appears at 12.82 ppm in **6**.[35] Also, the H1 and H2 resonances are separated by ~2.9 ppm (Table III, Figure 6) as compared to ~0.6 ppm observed with **6**[35] and other imidazole complexes of trivalent cobalt.[31b] The single hydrogen (H9) on the pyrimidine ring resonates at 9.39 ppm. Assignment of the NH and NH_2 peaks (both disappear on addition of D_2O) is supported by their positions in the NMR spectrum of the $[Co(dien)_2]^{3+}$ (dien = diethylenetriamine) complex in $(CD_3)_2SO$[47] and the intensity ratio. The ^1H NMR spectrum of **6**[35] contains an interesting doublet–triplet–doublet–triplet (dtdt) pattern for the four hydrogens of the two CH_2 groups that bridge the peptido nitrogen and the imidazole ring. The ^1H–^{13}C COSY spectrum of **6** demonstrates that the pattern arises from the four mutually coupled hydrogen atoms resonating at four distinctly different positions.[48] A somewhat different (ddtt) pattern is observed in the case of **3** (Figure 6), presumably due to alteration(s) in the relative disposition of the same four hydrogens in the chelate framework. The two CH_2 groups between the NH and NH_2 functions give rise to the peaks at 2.15 and 3.17 ppm, while the single CH_2 between the NH function and the pyrimidine ring exhibits a complicated AB pattern at 4.81/4.98 ppm. The signal at 3.37 ppm is due to water molecules of crystallization, and that at 2.50 ppm is due to residual protons in $(CD_3)_2SO$.

The ^{13}C NMR spectrum of **3** (Figure 6) exhibits 13 distinct resonances for the 13 carbon atoms of the ligand. A significant

Table III. Spectral Data

Electronic Absorption

complex	solvent	λ_{max},[a] nm (ϵ)
3	H_2O	530 sh (90), 350 (3200), 275 (7200)
	DMSO	530 sh (120), 350 sh (3000)
4	H_2O	530 sh (95), 350 (3300), 275 (7400)
	DMSO	530 sh (125), 350 sh (3000)
7[b]	H_2O buffer (pH 6.1)	550 (136), 400 sh, 324 (6500), 254 (13000)

Circular Dichroism

complex	solvent	λ_{max},[a] nm ($\Delta\epsilon$)
3	H_2O	520 (0.73), 380 (−1.28)

^1H NMR ($(CD_3)_2SO$, 293 K, δ from TMS) for Complex 3

2.15 (2 H), 2.25 (t, J = 12 Hz, 1 H), 2.42 (t, J = 12 Hz, 1 H), 2.81 (d, J = 14 Hz, 1 H), 3.17 (2 H), 3.84 (d, J = 14 Hz, 1 H), 4.49 (2 H), 4.81/4.98 (ABq, J_{AB} = 19 Hz, 2 H),[c] 5.71 (s, 1 H), 7.86 (s, 1 H), 8.63 (s, 1 H), 9.39 (s, 1 H)

^{13}C NMR ($(CD_3)_2SO$, 293 K, δ from TMS) for Complex 3

25.41, 40.87, 41.69, 55.74, 57.45, 116.51, 120.91, 137.07, 145.25, 157.04, 164.56, 167.79, 170.57

[a] Values quoted as liter per mole of cobalt per centimeter. [b] Reference 46. [c] The low-field peaks exhibit another coupling of J = 6 Hz.

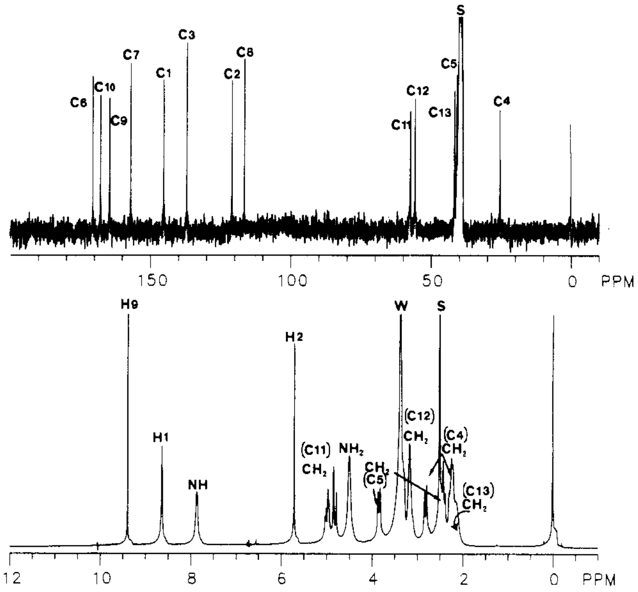

Figure 6. ^1H (lower trace) and ^{13}C (upper trace) NMR spectrum (300 MHz, 293 K) of $[Co(L)]_3Cl(BF_4)_2{\cdot}9.25H_2O$ (**3**) in $(CD_3)_2SO$. Signal assignments (see Figure 2) are indicated.

---

(47) Yoshikawa, Y.; Yamasaki, K. *Bull. Chem. Soc. Jpn* **1972**, *45*, 179.

(48) For more discussion and the values of the various coupling constants, see ref 26 and 35.

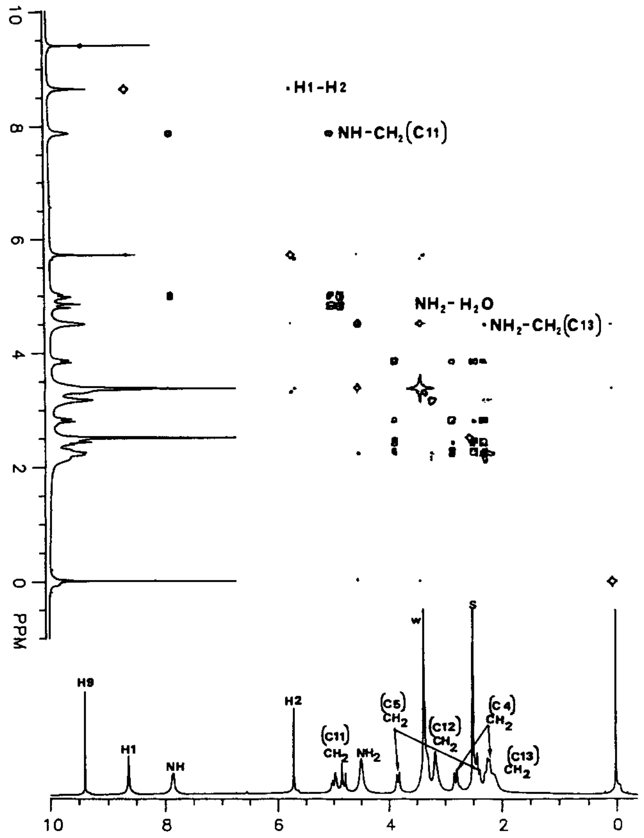

Figure 7. ^{1}H–^{1}H COSY spectrum of **3** in $(CD_3)_2SO$. Peaks due to water and residual protons in $(CD_3)_2SO$ are marked by W and S, respectively.

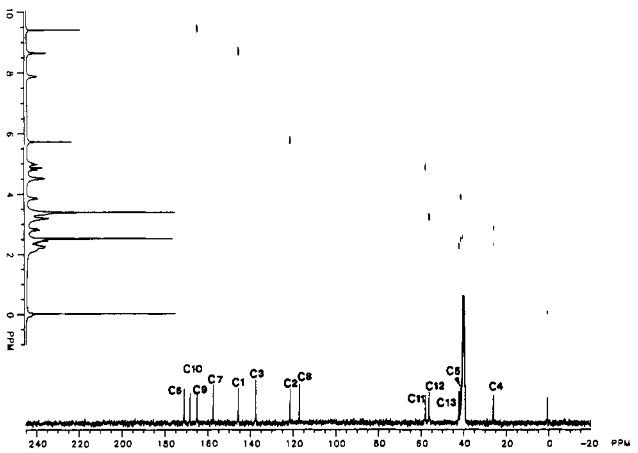

Figure 8. ^{1}H–^{13}C (J = 140 Hz) COSY spectrum of **3** in $(CD_3)_2SO$.

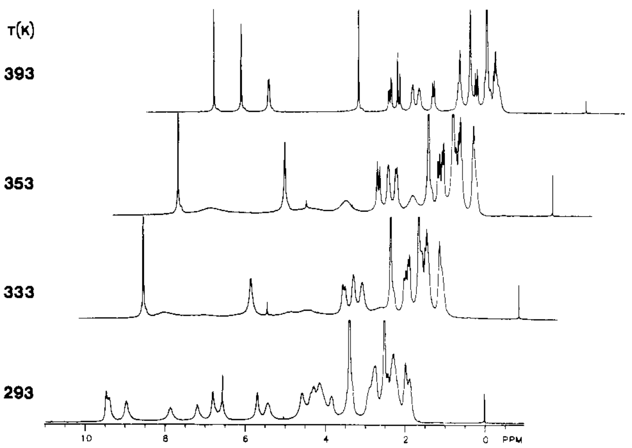

Figure 9. Variable-temperature ^{1}H NMR spectra of $[Co(L)]_4(BF_4)_4 \cdot 6H_2O$ (needle-shaped crystals of the tetramer[51]) in $(CD_3)_2SO$. The spectrum at the top is identical with the ^{1}H NMR spectrum of **3** at 393 K.[50]

number of peaks in this spectrum have been identified with the aid of the completely assigned NMR spectrum of **6**[35] and APT data. The peak corresponding to the carbonyl group (C6) moves from 167.28 ppm in PMAH (**2**) to 170.57 ppm in **3** as a result of coordination of the peptido nitrogen (N3) to cobalt. Similar downfield shift of the carbonyl resonance has been observed with **6** and other peptido complexes.[26,49] Formation of the imidazolate bridges between the cobalt centers in **3** results in a further downfield shift of the C1 resonance (145.25 ppm) as compared to the case of **6** (137.87 ppm) and the free ligand (134.53 ppm).[11] Assignments of the C1, C2, C4, C5, and C9 resonances rely on the ^{1}H–^{13}C COSY results (Figure 8), while the peaks corresponding to the pyrimidine ring carbons have been identified by comparing the ^{13}C NMR spectra of **3**, **2**, and **6**. Since both ^{1}H and ^{13}C NMR spectra of **3** (Figure 6) remain essentially unchanged[50] in the temperature range 293–393 K, it is evident that the trimeric structure of **3** undergoes minimal dynamic rearrangement(s) of the ligand framework in DMSO solution.

The ^{1}H–^{1}H and ^{1}H–^{13}C (J = 140 Hz) COSY spectra of **3** in $(CD_3)_2SO$ are shown in Figures 7 and 8, respectively. Inspection of these two figures reveals that (a) the hydrogen atoms on C4 and C5 in **3** exist as four distinct ones and they are all coupled to each other and (b) each CH_2 group (numbered C4 and C5) affords a set of one doublet and one triplet, thus giving rise to the "ddtt" pattern in the 2–4-ppm region. Figure 7 also illustrates a few other correlations. For example, the two imidazole hydrogens (H1 and H2) are weakly correlated. Since the water peak is strongly coupled to the NH_2 signal, it appears that, in $(CD_3)_2SO$ solution, few water molecules remain H-bonded to the NH_2 groups of the trimeric structure. The NH–CH_2 (C11) and NH_2–CH_2 (C13) connectivities are also clearly visible in Figure 7. Apart from the clue for the "ddtt" pattern, Figure 8 provides one with unambiguous assignments of the C1, C2, C9, C11, C12, and C13 resonances. Taken together, the NMR results indicate that Figure 2 does represent the solution structure of **3** quite as well.

An interesting aspect of the solution behavior of the macrocation of **4** must be mentioned here. At 293 K, **4** exhibits a rather unusual ^{1}H NMR spectrum (bottom trace, Figure 9).[51] This behavior is surprising, since the spectrum of **4** is expected to resemble that of **3** (Figure 6) very closely. Careful inspection of the 293 K spectrum of **4**, however, gives rise to the suspicion that the broad peaks might arise from slow tumbling of the large cation of **4** (mol wt ≈ 1700) in DMSO solution.[52] That indeed the unusual appearance of the spectrum at 293 K is due to sluggish molecular motion is confirmed by the sharpening of the peaks with rising temperature (Figure 9). The ^{1}H NMR spectrum of **4** merges into that of **3** at 393 K.[50] At this temperature, the ^{13}C NMR spectra of **3** and **4** are also interchangeable.

Summary. The following are the principal results and conclusions of this investigation.

(i) Two imidazolate-bridged Co(III) complexes (**3** and **4**) of PMAH (**2**), a "tailored" ligand that represents a major section of the metal-chelating portion of Bleomycin (BLM, **1**), have been synthesized and structurally characterized. Complex **3** is a chiral trinuclear species, while **4** is a symmetric tetranuclear complex. Both these complexes belong to a small class of polynuclear Co(III)

---

(49) (a) Boas, L. V.; Evans, C. A.; Gillard, R. D.; Mitchell, P. R.; Phipps, D. A. *J. Chem. Soc., Dalton Trans.* **1979**, 582. (b) Hawkins, C. J.; Martin, J. *Inorg. Chem.* **1986**, *25*, 2146.

(50) In addition to small shifts of the solvent peaks due to change in temperature, the NH_2 peak at ~4.5 ppm appears as a doublet at temperatures above 353 K.

(51) The needle-shaped crystals of the tetramer (see Experimental Section) analyze as $[Co(L)]_4(BF_4)_4 \cdot 6H_2O$. These crystals have been used for NMR experiments to avoid the DMF resonances.

(52) The viscosity of the DMSO solution is quite high at 293 K (DMSO freezes at 291 K). Several solvent molecules are also expected to be H-bonded to the complex cation, thereby giving rise to an effectively larger unit in solution.

complexes with imidazolate bridges.

(ii) The coordination structure around cobalt in either **3** or **4** approaches that proposed for the Co(III) complex of pseudotetrapeptide A of BLM.[46] Successful structure determination of **3** and **4** now clearly indicates the possibility of coordination of the pyrimidine, β-aminoalanine, and β-hydroxyhistidine moieties of BLM to cobalt in Co^{III}–BLM.

(iii) The identity of the sixth ligand that binds cobalt in orange Co^{III}–BLM has not been established. The present work strongly suggests that characterization of a series of complexes of the composition [Co(PMA)L]$^{n+}$ in which L denotes various ligands that represent other donor functions of BLM could eventually reveal the architecture of the coordination sphere of cobalt in orange Co^{III}–BLM.

Acknowledgment. Financial support from the donors of the Petroleum Research Fund, administered by the American Chemical Society, and a grant from the Cancer Research Coordination Committee of UC is gratefully acknowledged. We thank Jim Loo for help in the COSY experiments.

Supplementary Material Available: SPACFIL drawings of the cations in **3** and **4** (Figures S1 and S2), atomic coordinates and isotropic thermal parameters for the non-hydrogen atoms in **3** (Table S1) and **4** (Table S2), complete lists of bond lengths and angles for **3** (Tables S3 and S4) and **4** (Tables S7 and S8), anisotropic thermal parameters for **3** (Table S5) and **4** (Table S9), and H atom coordinates and isotropic thermal parameters for **3** (Table S6) and **4** (Table S10) (18 pages); values of $10|F_o|$ and $10|F_c|$ (Tables S11 and S12) (35 pages). Ordering information is given on any current masthead page.

Contribution from the Department of Chemistry, Massachusetts Institute of Technology, Cambridge, Massachusetts 02139, and Department of Radiology, Harvard Medical School and Brigham and Women's Hospital, Boston, Massachusetts 02115

Technetium Thiolate Complexes as Oxygen Atom Transfer Catalysts

Nadine de Vries,[1a] Alun G. Jones,[1b] and Alan Davison*,[1a]

Received February 16, 1989

Both Tc(III) compounds Tc(tmbt)$_3$(MeCN)$_2$ (**6**) and Tc(tmbt)$_3$(py)$_2$ (**7**) can be oxidized to Tc(V) oxo species by oxygen atom transfer. The initial product of the reaction of **6** with DMSO was characterized by X-ray crystallography and found to be Tc(tmbt)$_3$(DMSO)(MeCN), the product of ligand substitution, not oxygen atom transfer (crystal data: monoclinic, $a = 14.026$ (2) Å, $b = 26.856$ (7) Å, $c = 20.025$ (3) Å, $\beta = 104.20$ (1)°, space group = $P2_1/n$, $Z = 8$; final $R = 0.083$, $R_w = 0.105$). However, compound **6** is oxidized to TcO(tmbt)$_3$(py) (**1**) by pyridine *N*-oxide, and **7** reacts with a number of other oxygen atom transfer reagents as well to produce the oxotechnetium(V) complex **1**. The Tc(V) oxo compound TcO(SC$_{15}$H$_{23}$)$_3$(NC$_5$H$_5$) (**1**) was also characterized by X-ray crystallography (crystal data: monoclinic, $a = 13.487$ (2) Å, $b = 17.654$ (3) Å, $c = 21.603$ Å, $\beta = 96.676$ (9)°, space group = $P2_1/n$, $Z = 4$; final $R = 0.051$, $R_w = 0.064$). Addition of excess thiolate to **1** yields (Ph$_4$As)[TcO(tmbt)$_4$] (**3**), which can also be prepared directly from (Ph$_4$As)[TcOCl$_4$]. Both **1** and **3** can be reduced by oxygen atom abstraction to restore the Tc(III) tris(thiolate) core. Reaction of **3** with PEt$_3$ requires much more vigorous conditions than **1** does, but both materials are reduced to Tc(tmbt)$_3$(PEt$_3$)$_2$. The oxidative and reductive oxo-transfer reactions can be coupled to complete a catalytic cycle. In the oxidation of PPh$_3$ by DMSO, the catalyst is still fully active after 500 turnovers.

Oxygen atom transfer reactions of molybdenum have been extensively investigated because molybdoenzymes have been shown to catalyze reactions in which oxygen atoms are added or removed from substrates.[2] In contrast, the analogous chemistry of its neighbor, technetium, is essentially unexplored. Rare examples of such reactions include the removal of the oxo groups from both TcOCl$_2$(HB(pz)$_3$)[3] and [TcO(MoS$_4$)$_2$]$^{-}$[4] by phosphines, and Lu and Clarke have shown pyridine to act as an oxygen atom abstraction agent during the formation of μ-oxo dimers.[5]

Oxotechnetium complexes form a large part of the body of known technetium chemistry, mostly due to their use as diagnostic radiopharmaceutical agents,[6] and a significant number of these contain sulfur ligands.[7-10] We have recently reported the preparation of oxotechnetium(V) anions[11] as well as a series of Tc(III) compounds[12] that incorporate the sterically hindered ligands 2,3,5,6-tetramethylbenzenethiolate (tmbt) and 2,4,6-triisopropylbenzenethiolate (tibt). Conversion of one class of thiolate compound to the other formally involves the addition or removal of an oxygen atom and a concurrent change in the oxidation state of the metal of ±2. We have, therefore, studied the reactions of Tc(III) compounds with oxygen atom donor reagents and those of oxotechnetium(V) species with trialkyl- and triarylphosphines. These reactions and their application to catalysis are discussed herein.

Experimental Section

Caution! Technetium-99 is a weak β^--emitter ($E = 0.292$ MeV, $t_{1/2} = 2.12 \times 10^5$ years). All work has been done in laboratories approved for the use of low levels of radioactive materials. Precautions have been detailed elsewhere.[7]

Abbreviations used: Htmbt, 2,3,5,6-tetramethylbenzenethiol; Htibt, 2,4,6-triisopropylbenzenethiol.

Ammonium pertechnetate was supplied as a gift by Du Pont/Biomedical Products. The Tc(IV) complex, (NH$_4$)$_2$[TcCl$_6$], was prepared by the method of Nelson et al.,[13] and (Ph$_4$As)[TcOCl$_4$] and (n-Bu$_4$N)[TcOCl$_4$] were synthesized by the methods of Trop.[14] Reagents

---

(1) (a) Massachusetts Institute of Technology. (b) Harvard Medical School.

(2) Holm, R. H. *Chem. Rev.* **1987**, *87*, 1401.

(3) Abrams, M. J.; Davison, A.; Jones, A. G. *Inorg. Chim. Acta* **1984**, *82*, 125.

(4) DuPreez, J. G. H.; Gerber, T. I. A. *Inorg. Chim. Acta* **1985**, *110*, 59.

(5) Lu, J.; Clarke, M. J. *Inorg. Chem.* **1988**, *27*, 4761.

(6) Davison, A.; Jones, A. G. *Int. J. Appl. Radiat. Isot.* **1982**, *33*, 875.

(7) Davison, A.; Orvig, C.; Trop, H. S.; Sohn, M.; DePamphilis, B. V.; Jones, A. G. *Inorg. Chem.* **1980**, *19*, 1988.

(8) Byrne, E. F.; Smith, J. E. *Inorg. Chem.* **1979**, *18*, 1832.

(9) DePamphilis, B. V.; Jones, A. G.; Davison, A. *Inorg. Chem.* **1983**, *22*, 2292.

(10) Spies, H.; Johannsen, B. *Inorg. Chim. Acta* **1981**, *48*, 225.

(11) Davison, A.; de Vries, N.; Dewan, J.; Jones, A. G. *Inorg. Chim. Acta* **1986**, *120*, L15.

(12) de Vries, N.; Dewan, J. C.; Jones, A. G.; Davison, A. *Inorg. Chem.* **1988**, *27*, 1574.

(13) Nelson, C. M.; Boyd, G. E.; Smith, W. T., Jr. *J. Am. Chem. Soc.* **1954**, *76*, 348.

0020-1669/89/1328-3728$01.50/0